Discharge flow of a cohesive granular media from a silo

Adrien Gans, Blanche Dalloz-Dubrujeaud, Maxime Nicolas, Pascale Aussillous

Discharge flow of a cohesive granular media from a silo

Adrien Gans,[1,*] Blanche Dalloz-Dubrujeaud,[1] Maxime Nicolas,[1] and Pascale Aussillous[1,†]

[1] *Aix Marseille Univ, CNRS, IUSTI, Marseille, France*

(Dated: December 9, 2024)

Cohesion can dramatically affects the flow of granular media. In this paper, thanks to a cohesion-controlled granular material, we propose to investigate experimentally the effect of the cohesion on the discharge from a silo. We use two geometries, a cylindrical silo and a thin rectangular silo, with an adjustable bottom to control the size of the orifice. Similarly to cohesionless granular material, the mass flow rate is mostly controlled by the diameter of the outlet D, however we observe that the cohesion tends to decrease the flow rate. We show that this effect is controlled by a cohesive length, based on the cohesive yield stress and gravity acceleration, which acts as an effective particle size. This cohesive length is also found to control the onset of flow.

The discharge flow of a powder from a silo is very important for many industrial applications, for example when handling fine sand, cement, pharmaceutical powders and flours [1–3]. Indeed, fine particles tend to aggregate, and this cohesion may lead to ratholing, arching, irregular discharge or complete blockage[4]. Whereas many advances have been made in the description of cohesionless granular flows in various configurations [5] and in particular concerning the silo discharge [6–18], the behavior of cohesive powders remains elusive. One difficulty lies in the understanding of the cohesion force between the particles. For very small particles (typically below 10 μm in diameter), attractive forces like Van der Waals [19] or electrostatic forces [20] are dominant whereas for larger particles, humidity brings the necessary amount of water to build strong liquid bridges between particles and therefore creates a bulk cohesion [21]. Since the concept of cohesion is widely used with many influencing parameters (confinement pressure, temperature, humidity rate) or mechanisms (ageing, sintering, chemical reaction), there is a need of a simple definition and a good control of the cohesion to perform quantitative experiments. This was achieved recently by Gans *et al.* [22] who has developed a cohesion-controlled granular material where the cohesion originates from a polymer coating of glass particles. The adhesive interparticle force can then be tuned by controlling the thickness of the coating. This material has already been used to study the erosion of a cohesive granular bed by a turbulent jet [23] and the collapse of a cohesive granular column [24].

With this granular material with controlled cohesion, the objective of this Letter is to elucidate experimentally the role of cohesion on the discharge flow of a silo. We first focus on the flow threshold before studying how the cohesion affects the mass flow rate during the discharge of a cylindrical silo. Finally we investigate the effect of cohesion on the velocity profile at the outlet of a rectangular silo which was designed for imaging.

We used two experimental configurations which are shown in Fig. 1(a,b). Both silos are made of Perspex (PMMA) with an outlet located in the center of the bottom plate. We designed a set of removable bottom plates to change the size of the orifice, D, from 1 mm to 30 mm. The particles are made of glass beads of diameter $d = 340 \pm 50$ μm or $d = 800 \pm 60$ μm, with a particle density of $\rho = 2600$ kg·m^{-3}. The cohesion between particles is brought by a coating with a PBS polymer layer whose average thickness tunes the static cohesive stress, τ_c (see Gans *et al.* [22] for more details). A qualitative view of the cohesion is shown in Fig. 1(c). Following previous work [22, 24], the cohesion strength is characterized by a cohesion length ℓ_c given by the balance of the hydrostatic pressure and the cohesive stress:

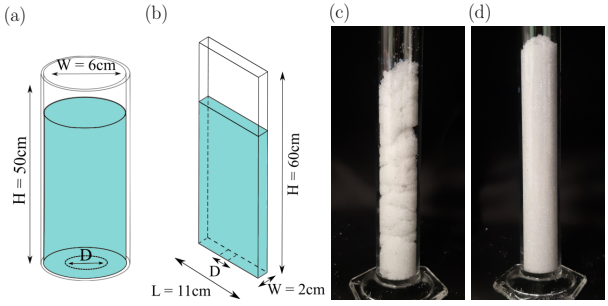

FIG. 1: Sketch of (a) the cylindrical and (b) the rectangular silo with their respective dimensions. Example of a highly cohesive granular material poured into a tube ($d = 340$ μm, $\ell_c = 10.6$ mm) (c) without and (d) with intense stirring in the funnel used during filling.

$$\ell_c = \frac{\tau_c}{\phi_b \rho g}, \tag{1}$$

where ϕ_b is the bulk volume fraction and g the acceleration of gravity. To obtain a discharge in the range of orifice diameters explored, the cohesive length was varied from 0 (dry granular) to a moderate value of $\ell_c = 2.6$ mm. The friction coefficient between cohesive grains and the PMMA walls was measured as $\mu_w = \tan(8.1 \pm 0.4^\circ)$ which ensured that the cohesive grains do not adhere to the silo walls. At the beginning of the experiment, the orifice is closed by a stopper and the cohesive material is poured in the silo using a funnel with a continuous stirring to obtain

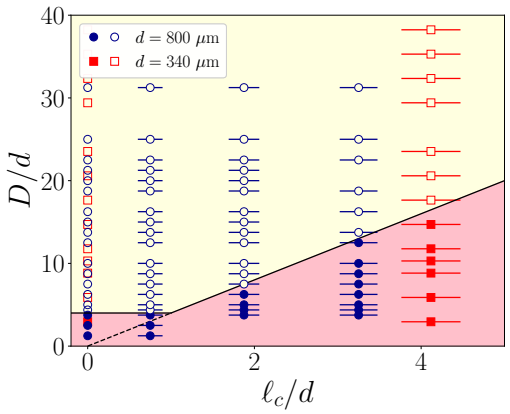

FIG. 2: Flowing map for the cylindrical silo depending on the cohesive length ℓ_c, the size of the grains d and the outlet diameter D. Empty symbols (and yellow background) stands for a flow of grains, whereas full symbols (and pink background) stands for no-flow.

a homogeneous volume fraction, as shown in Fig. 1(d). The height h_p of the column of grains and the mass m of particles gives the initial volume fraction of the material, $\phi_b = m/(\rho S_b h_p)$, where S_b is the area of the silo cross-section. In our experiments, ϕ_b varies between 0.55 and 0.60 depending slightly on ℓ_c [22, 25] (see Supplemental Material where data and plots are given [26]).

We first focus on the flow threshold for the cylindrical silo. Many past studies on the jamming of silo flows for dry granular material [27–33] showed that jamming is observed with the formation of an arch when the particle size is not very small compared to the outlet size, typically for $D \lesssim 4d$. In our study with a cohesive material, the flowing map of the cylindrical silo is drawn from repeated flow observations with the two batches of particles diameter with different cohesive lengths, ℓ_c, and different silo outlet diameter, D. The flowing map is presented in Fig. 2 where both lengths D and ℓ_c are normalised by the particle diameter. Empty symbols correspond to experiments where the flow occurs and full symbols to experiments where jamming is observed after the removal of the stopper. The dry granular flow threshold $D \approx 4d$ seems to hold even for weakly cohesive particles with $\ell_c/d < 1$ (see the horizontal line in the figure). For more cohesive particles ($\ell_c/d > 1$), the critical exit diameter clearly increases linearly with the cohesive length. To explain this result, we can consider the balance between gravity force and cohesion force at the interface for a cylindrical column of material, of height h, located above the orifice:

$$\phi_b \rho g h S \simeq \tau_c h \mathcal{P} \tag{2}$$

where S and $\mathcal{P}$ are the area and the perimeter of the outlet. This equation can be rewritten for the cylindrical silo as $D \simeq 4\ell_c$, and is used to draw the line separating the flow area (yellow) and the no-flow area (pink) in Fig. 2 in good agreement with the experimental data. This suggests that the cohesion length plays the same role as the grain size for cohesionless particles. Given this result, we introduce an effective size corresponding to the maximum length between the cohesion length and the grain diameter:

$$d^* = max[d, \ell_c]. \tag{3}$$

The flow condition for the cylindrical silo is now given, for all materials, by:

$$D \gtrsim 4d^*. \tag{4}$$

We now focus on the role of cohesion on the discharge flow-rate. The discharge flow-rate of a dry granular media from a silo has been widely studied since the pioneer work of Hagen in 1852 [6] (translated in [34]). During the discharge, it is well known that the flow rate is constant and does not depends of the quantity of material in the silo. This behaviour was first explained by Hagen [6] introducing the concept of a free fall arch at the outlet which scales with the outlet size D. This gives a velocity at the outlet scaling as $v_c \propto \sqrt{gD}$ and a mass flow rate,

$$Q = c\rho S\sqrt{gD}. \tag{5}$$

Recently, it has been shown that instead of a free fall zone, an acceleration zone develops at the outlet [12]. Moreover, continuum modeling simulations using the shear-dependent frictional rheology $\mu(I)$ [35–37] succeeded to reproduce the experimental observations for different geometries [9, 11, 14–18]. These studies suggest that close to the outlet, the inertial force dominates the flow and the friction force becomes negligible, in line with the scaling of the free-falling arch concept.

During the discharge, we measured the flow-rate with a connected accurate weight-scale. The flow rate was found to be steady, as in the cohesion-less case. Fig. 3(a) shows the mass flow-rate versus the diameter of the outlet D in a log-log plot, for the cylindrical silo. The data mainly follows the classical law given by equation 5 (see the black dashed lines) which shows that the outlet diameter is the main parameter controlling the mass flow rate, whether the material is cohesive or not. This significant finding demonstrates the universality of the mechanism regulating the flow of granular media through an opening.

For dry granular materials, particle size is known to play a second-order role in controlling mass flow, as first described by Hagen [6] and Beverloo *et al.* [7]. They proposed to consider a reduced exit diameter $(D-kd)$ where k is a fitting parameter. This leads to the widely used empirical expression for the discharge of a flat-bottomed silo, known as "Beverloo's law", which implies that the data can be rescaled using the dimensionless outlet diameter D/d. In Fig 3(b), we then plot the flow rate made dimensionless by using the main power law, $Q/\phi_b\rho S\sqrt{gD}$,

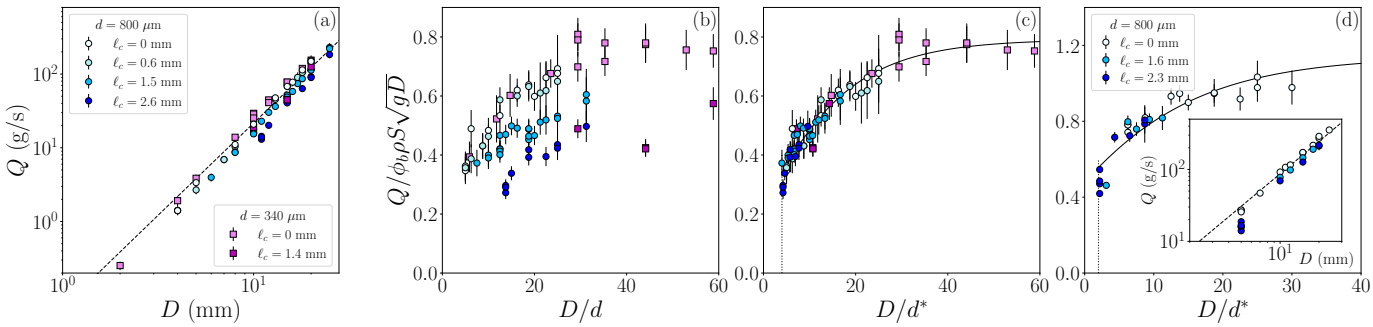

FIG. 3: (a) Mass flow rate and (b,c) dimensionless mass flow rate versus (a) the outlet diameter D, (b) D/d and (c) D/d^*, for the cylindrical silo and several cohesions. (d) Dimensionless mass flow rate versus D/d^* for the rectangular silo (inset: mass flow rate versus D). The dashed line represents equation 5 with (a) $c = 0.34$ and (inset of d) $c = 0.53$. The black line represents equation 6 with $\beta = 0.08$ and (c) $C = 0.79$, $\alpha = 0.47$ and (d) $C = 1.14$, $\alpha = 0.35$. The dotted vertical line represents the flow threshold.

versus D/d. As expected, the data shows a good collapse for the dry cases ($\ell_c = 0$). For the cohesive cases, we observe that weakly cohesive particles, with $\ell_c/d < 1$, behave like dry granular media (data are superimposed with the dry cases for $d = 800\mu$m, $\ell_c = 0.6$mm) whereas for more cohesive particles ($\ell_c/d > 1$), the dimensionless flow-rate decreases with increasing cohesive length. Despite the moderate cohesion range studied, the flow rate can be reduced by a factor of 2. All this suggests that, as with the flow threshold, the effective size d^* (given by eq. 3) may simply play the same role as particle size.

To assess this hypothesis, we plot in Fig. 3(c) the dimensionless flow-rate, $Q/(\phi_b\rho S\sqrt{gD})$, versus D/d^* for the cylindrical silo. All the data collapse, suggesting that the cohesive length, which is derived from the internal cohesive stress, is representative of an inner characteristic scale for the material and acts as an effective particle size for $\ell_c > d$. To elucidate the origin of this behaviour, it would be valuable to conduct DEM simulations and investigate the role of cohesion on the statistics of force chains network and on the possible formation of transient clustering in these flows, which might behave as virtual particles of larger size.

We can therefore use the recent formalism developed to describe the discharge of dry granular media from a silo. Indeed, using a mono-layer experiment, Janda *et al.* [8] challenged the concept of a "useless zone" for particles near the outlet walls proposed by Beverloo *et al.* [7]. They found that the velocity and density profiles at the outlet are self-similar, which allows to deduce the flow rate, $Q \propto \rho\phi_c v_c$, from the values v_c and ϕ_c of the velocity and the volume fraction at the center of the outlet. They then observed that for small outlet sizes, the granular packing tends to dilate, explaining the decrease in flow-rate. On the basis of this work, Benyamine *et al.* [10] showed that this dilation depends on the ratio D/d and proposed an empirical relationship, $\phi_c \propto \phi_b\left[1 - \alpha e^{-\beta D/d}\right] = \phi_b G(D/d)$ where α and β are fitting parameters. Using discrete element simulations, Zhou *et al.* [13] showed that the particle size has a similar influence on the velocity at the outlet, following $v_c \propto \sqrt{gD}G(D/d)$, which seems consistent with a continuous description of the granular media with a shear-dependent volume fraction. The flow-rate is then given by $Q = C\rho\phi_b S\sqrt{gD}G^2(D/d)$ with a fitting parameter C. We propose to use this equation with d^* instead of d:

$$Q = C\phi_b\rho S\sqrt{gD}\left[1 - \alpha e^{-\beta D/d^*}\right]^2. \qquad (6)$$

The best fit of Eq. 6 using the least squares method provides a good agreement with the data in Fig. 3(c) for $C = 0.79$, $\alpha = 0.47$ and $\beta = 0.08$ (see the black line). These values are similar to those obtained by Benyamine *et al.* [10]. The dotted vertical line in Fig. 3(c,d) corresponds to the flow threshold (Eq.4).

The same behaviour is recover for the rectangular silo (Fig. 3d): The flow-rate is mainly controlled by the outlet diameter (see the dashed line in the inset), and a good collapse of the data is obtained by plotting the dimensionless flow rate, $Q/\phi_b\rho S\sqrt{gD}$, versus D/d^*. The dotted vertical line corresponds to the flow threshold, $D \simeq 2d^*$, assuming that $\mathcal{P} = 2W$ as the grains slide on the wall. The data are fairly well adjusted by equation 6, with the fitting parameters values $C = 1.14$, $\alpha = 0.35$ and $\beta = 0.08$ (see the black line in Fig. 3d) similar to previous works [8, 10, 13]. Note that we keep the same value for β as in the cylindrical case (in [10], β does not seem to depend on the geometry, contrary to α and C which shows that this empirical law as well as Beverloo's law are not yet universal).

Eq. 6 assumes that both the velocity and volume fraction at the center of the outlet depend slightly on the effective particle size d^*. To study the velocity field near the orifice, the flow was recorded in the rectangular

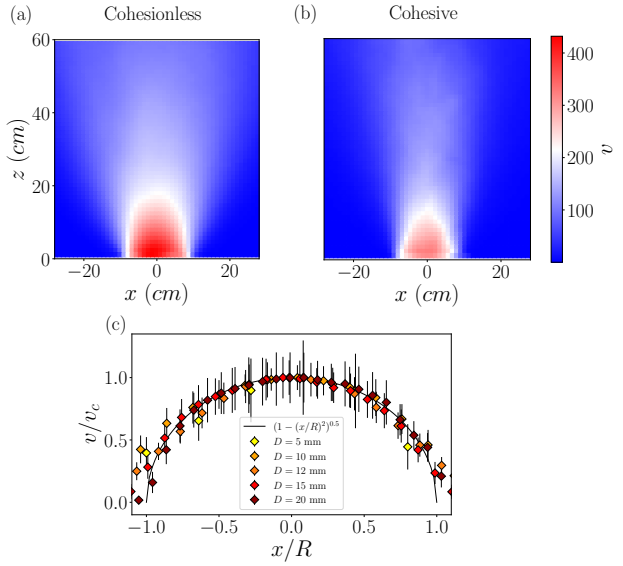

FIG. 4: Velocity field in the vicinity of the outlet for $D = 20$ mm, $d = 800$ μm and (a) cohesionless grains, (b) cohesive grains with $\ell_c = 1.6$ mm. (c) Velocity profile at the outlet $v(x)$ normalised by the velocity at its center, v_c for several orifice sizes D for $\ell_c = 2.3$ mm.

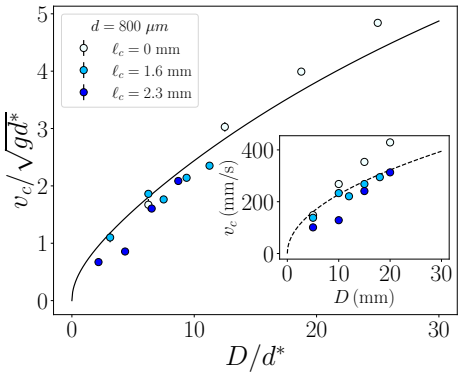

FIG. 5: Normalised velocity at the center of the outlet, $v_c/\sqrt{gd^*}$, versus the normalised outlet size D/d^* for several cohesion. Inset: velocity at the center versus the outlet size. The dashed line represents $\xi_0\sqrt{gD}$, and the line Eq. 7 with $\xi_0 = 0.73$, $\xi = 0.92$, $\alpha = 0.35$, $\beta = 0.08$.

silo using a high-speed camera. Particle velocities were measured by particle image velocimetry (PIV) using the Python toolbox OPENPIV, with a square interrogation region of 32 pixels, and an averaging over 2000 pairs of consecutive images during the steady-state discharge period. Examples of velocity profiles are shown in Fig. 4 for (a) cohesionless grains and (b) cohesive grains. We observe that in the cohesive case the flow is more channelled and the velocity at the center is about 25% lower than in the dry case. However, the velocity profile is found to be self-similar following exactly the same profile as the cohesionless media [8, 13] as shown in Fig. 4(c). The velocity v_c at the center of the outlet is plotted in Fig. 5. In the inset, we observe that, as expected, it is mainly controlled by the outlet size D (see the dashed line corresponding to $v_c \propto \sqrt{gD}$). However, as the cohesion increases, the velocity decreases slightly. Since the cohesion length is an effective size of the system,we plot in Fig. 5 the velocity as a function of the outlet size both made dimensionless using d^* as the characteristic length. The collapse of the data is fairly good, considering that the profile is taken at the wall, and it is well fitted by

$$v_c = \xi\sqrt{gD}\left[1 - \alpha e^{-\beta D/d^*}\right], \qquad (7)$$

using $\alpha = 0.35$, $\beta = 0.08$ and with $\xi = 0.92$ the only fitting parameter (see the black line).

Although very simple, the silo discharge setup reveals many important features of a granular material. Our cohesion-controlled granular media is characterised by a cohesive length ℓ_c derived from the internal cohesive stress. We have shown that this cohesive length is representative of an inner characteristic scale for the material. Indeed, thanks to a force balance, we have first shown that the flow threshold depends on an effective particle size $d^* = max[\ell_c, d]$ that describes both cohesive and cohesionless granular materials. Then, during the discharge, the flow-rate is mainly governed by the size of the orifice, whether the material is cohesive or not, which indicates the generality of the mechanism that controls the flow through an opening. Remarkably, the exit velocity profiles show no significant difference between cohesive and cohesionless materials, which underlines this generality. As with cohesionless granular flows, the velocity at the center of the orifice scales mainly with the square root of the outlet size [8], with a weak effect from the cohesive length. Following [13], this effect can be implemented through a geometrical factor $G(D/d^*) = \left[1 - \alpha e^{-\beta D/d^*}\right]$, where the particle diameter is replaced by the effective diameter d^*. The flow-rate is well fitted by assuming $Q \propto \rho\phi_b S\sqrt{gD}G^2(D/d^*)$, which suggests that the volume fraction at the center of the outlet should also depend similarly on d^*. These results confirm that, despite the apparent complexity of the cohesion phenomenon, the cohesion length simply acts as an effective particle diameter. Conversely, these results could also mean that the role of particle diameter in the discharge flow of a silo may be due to the distribution of internal stresses. Performing DEM simulations would be useful for gaining insight into these important observations which could help to develop continuum models to describe and understand silo discharge flow, whether the material is cohesive or not. It provides solid evidence that a cohesive rheology could be defined as has been done in other geometries [38, 39] and may represent a significant step towards understanding powder flows.

The authors thank O. Pouliquen and P.-Y. Lagrée for fruitful discussions. This work was supported by the ANR Grant No. ANR- 17-CE08-0017 under COPRINT (Cohesive Powders Rheology: Innovative Tools) project.

* Present Address: Université de Lorraine, CNRS, LEMTA, Vandœuvre-lès-Nancy, France
† pascale.aussillous@univ-amu.fr

[1] D. Geldart and J. Williams, Powder Technology **43**, 181 (1985).
[2] A. Cannavacciuolo, D. Barletta, G. Donsì, G. Ferrari, and M. Poletto, Powder Technology **191**, 272 (2009).
[3] D. Barletta, G. Donsì, G. Ferrari, M. Poletto, and P. Russo, AIChE Journal **53**, 2240 (2007).
[4] D. Schulze, *Powders and Bulk Solids* (Springer Berlin, Heidelberg, 2007).
[5] B. Andreotti, Y. Forterre, and O. Pouliquen, *Granular Media: Between Fluid and Solid* (Cambridge University Press, 2013).
[6] G. Hagen, Bericht über die zur Bekanntmachung geeigneten Verhandlungen der Königlich Preussischen Akademie der Wissenschaften zu Berlin , 35 (1852).
[7] W. A. Beverloo, H. A. Leniger, and J. Van de Velde, Chemical engineering science **15**, 260 (1961).
[8] A. Janda, I. Zuriguel, and D. Maza, Phys. Rev. Lett. **108**, 248001 (2012).
[9] L. Staron, P.-Y. Lagrée, and S. Popinet, Phys. Fluids **24**, 103301 (2012).
[10] M. Benyamine, M. Djermane, B. Dalloz-Dubrujeaud, and P. Aussillous, Phys. Rev. E **90**, 032201 (2014).
[11] L. Staron, P.-Y. Lagrée, and S. Popinet, The European Physical Journal E **37**, 1 (2014).
[12] S. Rubio-Largo, A. Janda, D. Maza, I. Zuriguel, and R. Hidalgo, Phys. Rev. Lett. **114**, 238002 (2015).
[13] Y. Zhou, P. Ruyer, and P. Aussillous, Phys. Rev. E **92**, 062204 (2015).
[14] S. Dunatunga and K. Kamrin, Journal of Fluid Mechanics **779**, 483 (2015).
[15] G. Daviet and F. Bertails-Descoubes, Journal of Non-Newtonian Fluid Mechanics **234**, 15 (2016).
[16] Y. Zhou, P. Y. Lagrée, S. Popinet, P. Ruyer, and P. Aussillous, Journal of Fluid Mechanics **829**, 459 (2017).
[17] Z. Zou, P. Ruyer, P.-Y. Lagrée, and P. Aussillous, Phys. Rev. E **102**, 052902 (2020).
[18] Z. Zou, P. Ruyer, P.-Y. Lagrée, and P. Aussillous, Phys. Rev. Fluids **7**, 064306 (2022).
[19] A. Castellanos, Advances in Physics **54**, 263 (2005).
[20] L. Konopka and J. Kosek, Journal of Electrostatics **87**, 150 (2017).
[21] L. Bocquet, E. Charlaix, S. Ciliberto, and J. Crassous, Nature **396**, 735 (1998).
[22] A. Gans, O. Pouliquen, and M. Nicolas, Phys. Rev. E **101**, 032904 (2020).
[23] R. S. Sharma, M. Gong, S. Azadi, A. Gans, P. Gondret, and A. Sauret, Phys. Rev. Fluids **7**, 074303 (2022).
[24] A. Gans, A. Abramian, P.-Y. Lagrée, M. Gong, A. Sauret, O. Pouliquen, and M. Nicolas, Journal of Fluid Mechanics **959**, A41 (2023).
[25] J. Fiscina, G. Lumay, F. Ludewig, and N. Vandewalle, Physical review letters **105**, 048001 (2010).
[26] See Supplemental Material at http:// for the data and data analysis.
[27] K. To, P.-Y. Lai, and H. K. Pak, Phys. Rev. Lett. **86**, 71 (2001).
[28] I. Zuriguel, A. Garcimartín, D. Maza, L. A. Pugnaloni, and J. M. Pastor, Phys. Rev. E **71**, 051303 (2005).
[29] L. Pournin, M. Ramaioli, P. Folly, and T. M. Liebling, The European Physical Journal E **23**, 229 (2007).
[30] A. Janda, I. Zuriguel, A. Garcimartín, L. A. Pugnaloni, and D. Maza, Europhysics Letters **84**, 44002 (2008).
[31] A. Janda, D. Maza, A. Garcimartín, E. Kolb, J. Lanuza, and E. Clément, Europhysics Letters **87**, 24002 (2009).
[32] D. Gella, D. Maza, I. Zuriguel, A. Ashour, R. Arévalo, and R. Stannarius, Phys. Rev. Fluids **2**, 084304 (2017).
[33] A. Nicolas, A. Garcimartín, and I. Zuriguel, Phys. Rev. Lett. **120**, 198002 (2018).
[34] B. P. Tighe and M. Sperl, Granular Matter **9**, 141 (2007).
[35] G. MiDi, The European Physical Journal E **14**, 341 (2004).
[36] P. Jop, Y. Forterre, and O. Pouliquen, Nature **441**, 727 (2006).
[37] Y. Forterre and O. Pouliquen, Annu. Rev. Fluid Mech. **40**, 1 (2008).
[38] S. Mandal, M. Nicolas, and O. Pouliquen, Phys. Rev. X **11**, 021017 (2021).
[39] A. Abramian, L. Staron, and P.-Y. Lagrée, Journal of Rheology **64**, 1227 (2020).